

**P.J. Stuttaford, P.A. Rubini. "Assessment of a radiative heat transfer model for a new gas turbine combustor preliminary design tool". AIAA J. Propulsion & Power, Vol. 14, No. 1, Jan-Feb 1998, pp. 66-73**

# ASSESSMENT OF A RADIATIVE HEAT TRANSFER MODEL FOR A NEW GAS TURBINE COMBUSTOR PRELIMINARY DESIGN TOOL

**Peter J. Stuttaford<sup>#</sup> and Philip A. Rubini<sup>\*</sup>**

School of Mechanical Engineering, Cranfield University, Bedford, MK43 0AL, England

## Abstract

Preliminary gas turbine combustor design presents a challenging process of analytical analysis and rig testing. The objective of this work is the development of a versatile radiation model for an existing preliminary gas turbine combustor design tool, able to model all conceivable combustor types. A network approach forms the basis of the design solution algorithm, dividing the domain into a number of independent semi-empirical interconnected sub-sections. A pressure-correction scheme solves the continuity equation and a pressure-drop/flow-rate relationship. A full conjugate heat transfer analysis allows the calculation of flametube heat loss. Radiation represents the most difficult mode of heat transfer to simulate in the combustor environment. A discrete transfer radiation model is developed and validated for use within the network solver. The effect of the new radiation model on the prediction of liner wall temperature is evaluated in an annular gas turbine combustor. The importance of radial distributions of temperature and soot are evaluated by examining the flametube wall heat transfer mechanism.

---

<sup>#</sup> Graduate Research Assistant. AIAA member.

<sup>\*</sup> Lecturer. Corresponding author.

## Nomenclature

$C_p$  = specific heat at constant pressure

$C_0$  = soot index of refraction constant

$C_2$  = Planck's second constant = 0.0143879 mK

$d$  = external mass flow into node

$dA$  = surface area associated with ray origin

$E$  = energy source term

$f_v$  = soot volume fraction

$h$  = convective heat transfer coefficient

$I$  = radiative intensity

$I_w$  = incident radiative intensity

$k_a$  = absorption coefficient

$k_s$  = scattering coefficient

$K$  = extinction coefficient

$\dot{m}$  = mass flow rate

$P$  = pressure

$q_+$  = outgoing radiative flux

$q_-$  = incident radiative flux

$Q$  = volumetric flow rate

$R$  = conductive heat transfer coefficient

$s$  = distance

$\Delta s$  = ray volume pathlength

$T$  = temperature

$\eta_l$  = emissivity

$\phi$  = azimuthal angle

$\theta$  = polar angle

$\rho$  = density

$\sigma$  = Stefan-Boltzman constant

$\Omega$  = ray solid angle

### Subscripts

$f$  = film

$g$  = gas

$n$  = entering volume element

$n+1$  = leaving volume element

$s$  = soot

$T$  = total

$w$  = wall

## **Introduction**

Gas turbine combustor development involves a lengthy process of analysis, beginning with the conception of overall performance requirements. Given an idea of the sizing requirements of a combustor, a basic geometrical layout may be developed providing the first step to detailed empirically based design validation, followed by more complex computational fluid dynamics (CFD) simulations and rig testing. Many of today's new combustors are extensions of well proven designs, and modified scale versions of these designs provide the first pass for the design validation procedures.

Semi-empirical models have the advantage of rapid execution times, on the order of a few minutes or less. This is an advantage for the design engineer as it allows optimisation with relatively little time expenditure. The more accurate this initial design process the more rapid the following phases of design. The limitations of such tools include their restriction to simple geometries; being cumbersome to set-up and having difficulties with convergence when applied to more irregular flow fields. Network methods have the ability to model complicated and unusual geometries effectively and with little numerical difficulty while retaining the advantage of rapid execution.<sup>1</sup>

A network consists of a number of independent sub-flows linked together to model a physical process. The method has been used with success in modelling large pipe networks.<sup>2</sup> Since the orientation of the sub-flows are independent, multi-dimensional features such as total-static fed cooling rings may be modelled with ease. Each sub-flow is defined by a semi-empirical pressure-drop/flow rate relationship and a heat transfer relationship.

Radiation represents the most difficult mode of heat transfer to simulate in the combustor environment. Previous comparisons, using a simplified heat transfer approach have shown qualitative agreement but highlighted the need for a more broadly applicable radiation

procedure.<sup>1</sup> An effort is made to extend the predictive radiative capability of the code beyond simple conventional empirical radiation correlations, improving the flexibility and accuracy of the radiation calculation to that of the underlying network solver.

### **Radiation**

Radiation is governed by a complex integrodifferential equation, which must be simplified to solve economically. Radiative heat transfer from the flame and combustion products to the surrounding walls may be computed given knowledge of the radiative properties and temperature distributions within the medium. However, these requirements are generally unknown and therefore the total energy and radiative energy conservation equations must be coupled.

A number of solution strategies exist for radiative heat transfer. The simplest make use of semi-empirical correlations to simulate the radiation in a one-dimensional domain.<sup>3</sup> The application of these models require sweeping assumptions concerning system geometry, gas temperature and radiative properties. The accuracy of the correlations is limited within complex geometries and at elevated pressures, regimes beyond those used to originally formulate the relationships.

More complex models take direct account of the geometry. A balance must be made between solution accuracy and solution economy.<sup>4,5</sup>

Statistical methods such as the Monte Carlo scheme provide solutions approaching those of the exact solution.<sup>6</sup> The method has been successfully employed in complex geometries and accounts for spectral effects. A factor limiting the use of this method is the excessive computational time required for practical engineering calculations.

The zonal method has been widely used for solutions to practical problems.<sup>6</sup> Direct exchange area factors between the surface and volume elements must be computed, and the total exchange area calculated. This becomes a time consuming task as the geometry increases in complexity. A further difficulty arises for an absorbing and emitting medium as the attenuation of radiation along a path connecting area elements must be accounted for in the calculation of exchange areas.

Radiation intensity is dependent upon location, the direction of radiation propagation, and wavelength. The problem is complicated by the angular dependence of the intensity. If the assumption is made that the intensity is uniform over specified solid angles the problem may be simplified, and the integrodifferential radiative transfer equation is reduced to a series of coupled linear differential equations. This procedure forms the basis of the flux methods.<sup>6</sup> They include multiframe models, moment methods, spherical harmonics ( $P_N$ ) approximations, and discrete-ordinate models. Essentially, they only differ in the derivation of weighting coefficients for the intensities in each direction. Although these methods provide accuracy with computational economy they involve mathematical complexity.

Hybrid solution strategies combine the best of existing models. The discrete transfer method is such a model, combining elements of the zonal, Monte Carlo, and discrete ordinate methods.<sup>7</sup>

## **Radiation in Gas Turbine Combustors**

A large proportion of the heat transferred to the liner wall from the hot combusting gases and particles within the combustor flametube is by radiation. It follows therefore that an accurate liner heat balance may only be performed with the assistance of a reliable radiation model.

Predictions of radiative flux are dependent upon the distribution of gas temperature and radiative properties. A number of examples exist of the implementation of radiation models to compute radiative flux in gas turbine combustors. Rizk and Mongia were able to achieve satisfactory wall temperature results using simple semi-empirical correlations for radiative transfer in a gas turbine combustor.<sup>8</sup> The correlations were implemented as part of a three-dimensional analysis. Menguc et al successfully employed a spherical harmonics ( $P_1$  and  $P_3$ ) model on a cylindrical enclosure at gas turbine combustor conditions.<sup>9</sup> It was necessary to make some assumptions in obtaining a soot concentration profile, allowing the effects of differing profiles to be evaluated.

Carvalho et al presented a three-dimensional model of a 'can' combustion chamber.<sup>10</sup> The discrete transfer method was employed to model the radiative transfer within the can. A simple conjugate heat transfer scheme was coupled to the CFD solution to directly calculate wall temperatures from the computed internal heat fluxes.

Bai and Fuchs performed a numerical analysis of the radiative heat transfer in the reacting flow of a gas turbine combustor.<sup>11</sup> The discrete transfer method was used to compute the radiative heat source terms. The mean temperature profile exhibited errors of upto 10% when the effects of radiation were neglected. The effect of turbulent temperature fluctuations in the heat radiation were also evaluated. As expected the turbulent fluctuations were significant where there were very large amplitude fluctuations. The mean values of

temperature presented a reasonable approximation when the levels of temperature fluctuation were globally low.

### **The Network Algorithm**

The domain of interest is modelled by overlaying a network on the system geometry. The network consists of a number of elements and nodes. The elements represent actual physical features in the domain, e.g. duct sections, holes, etc. The nodes join the elements to one another, thus combining independent features into a meaningful overall structure. The overall governing equations are solved within the nodes, while semi-empirical relationships may be employed to describe the flow through an element.

The procedure used for obtaining a solution to the flow equations is based upon a pressure correction methodology. The one-dimensional flow may be compressible or incompressible. The overall governing flow equations are the continuity equation, and a pressure-drop/flow rate relationship.<sup>2</sup> The continuity equation may be specified as,

$$\sum_{j=1}^J \rho_{i,j} Q_{i,j} s_{i,j} = -d_i \quad i = 1, 2, \dots, J \quad (1)$$

and the pressure-drop/flow-rate relationship as,

$$\Delta P_{i,j} = P_{n_{i,j}} - P_i = s_{i,j} \frac{Q_{i,j}}{|Q_{i,j}|} g_{i,j}(\rho_{i,j}) f_{i,j}(|Q_{i,j}|) \quad (2)$$

where,

$s_{i,j} = 1$  if the flow is in the positive direction

$s_{i,j} = -1$  if the flow is in the negative direction.

The functional relationships are derived from semi-empirical formulations for combustor features and internal flows. The nomenclature is illustrated in Fig. 1. below. The relationships are written as coefficients in the overall solution matrix, and simultaneously solved using a direct method.<sup>2</sup>

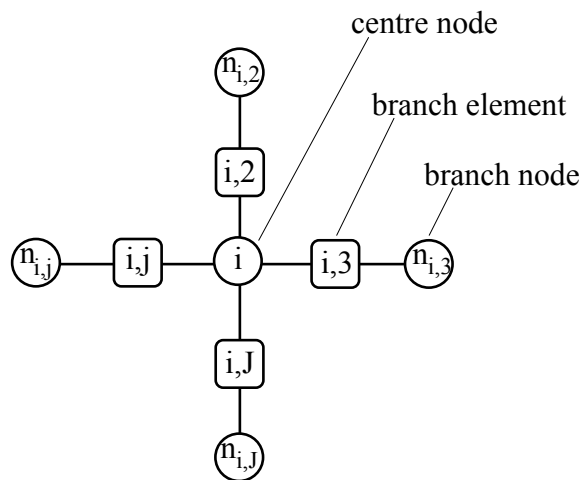


**Figure .1. Network Nomenclature**

The energy equation is satisfied by ensuring an enthalpy balance at each node within the network. This may be specified at nodes with branch elements containing mass transfer as,

$$T_i = \frac{\sum_{j=1}^J \left( E_{i,j} + \dot{m}_{i,j} C_p T_{n_{i,j}} \right)_{\text{inflow bits}}}{\sum_{j=1}^J \left( \dot{m}_{i,j} C_p \right)_{\text{inflow bits}}} \quad (3)$$

A semi-implicit formulation is used to compute node temperatures on boundaries or within walls, i.e. at nodes where the branch elements contain no mass flow. On the flow boundaries, where conduction, convection and radiation are present, this may be expressed as,

$$T_i = \frac{\left[ \sum_{j=1}^J R_{i,j} T_{n_{i,j}} \right]_{\text{conduction}} + \left[ \sum_{j=1}^J h_{i,j} T_{n_{i,j}} \right]_{\text{convection}} + \left[ (\varepsilon q_-)_i \right]_{\text{radiation}}}{\left[ \sum_{j=1}^J R_{i,j} \right]_{\text{conduction}} + \left[ \sum_{j=1}^J h_{i,j} \right]_{\text{convection}} + \left[ (\varepsilon \sigma T^3)_i \right]_{\text{radiation}}} \quad (4)$$

and within the solid where conduction is the only mode of heat transfer,

$$T_i = \frac{\left( \sum_{j=1}^J R_{i,j} T_{n_{i,j}} \right)_{\text{conduction}}}{\left( \sum_{j=1}^J R_{i,j} \right)_{\text{conduction}}} \quad (5)$$

The heat transfer coefficients in Eq. 4. are evaluated using semi-empirical correlations and data for various cooling types found in gas turbine combustors. The effect of film cooling has a significant effect on the wall temperatures, and must be modelled accurately. The calculations take the form of Nusselt number correlations, employing numerous experimental data. A wide range of cooling effects are modelled, including Z-rings, lipped-rings, slots,

effusion patches and transply patches. Heat pick-up by the fluid moving through the flametube wall is computed. Multiple films at the same location, originating from different features, are accounted for when computing the effective heat transfer coefficient. A constrained equilibrium calculation is used to obtain a mean flametube combustion gas temperature.

Further details of the network methodology may be found in Stuttaford and Rubini.<sup>1</sup>

### **The Discrete Transfer Radiation Model**

The discrete transfer (DT) method combines the advantages of other radiation procedures to provide a numerically exact and flexible solution algorithm. It allows for simple coupling to the existing overall flow and heat transfer solver. A further important advantage is the ease with which radiation properties models can be incorporated into the DT calculation.

DT involves tracing representative rays from one surface to another through the region of interest. An intensity distribution is calculated along each ray as it passes through the domain. The nature of radiation requires that this be a three-dimensional procedure. The intensities of the individual rays are summed at the various wall locations to give the net radiative heat flux. The accuracy of the calculation will obviously depend upon the number of rays projected at each point. The more complex the geometry and flowfield within the domain, the more rays that will be required to describe the radiative transfer through the domain. A disadvantage of the DT method is that too few rays may miss important information within the domain or on the boundary geometry. This is known as the 'ray effect'. Large numbers of rays may be required to accurately predict the radiative transfer in complex domains.

The transfer equation for thermal radiation along a ray in a direction  $s$  may be written as,<sup>7</sup>

$$\frac{dI}{ds} = -(k_a + k_s)I + k_a \frac{E_g}{\pi} + \frac{k_s}{4\pi} \int_{4\pi} P(\Omega, \Omega') I(\Omega') d\Omega' \quad (6)$$

where,

$$E_g = \sigma T_g^4$$

$P(\Omega, \Omega')$  = probability that the incident radiation in the direction  $\Omega'$  will  
scattered into the increment of solid angle  $d\Omega$  about  $\Omega$

Diameters of soot particles in hydrocarbon flames typically range in diameter between approximately  $0.005\mu\text{m}$  and  $0.3\mu\text{m}$ .<sup>4</sup> Using Mie theory the scattering cross section is a function of  $(\pi D/\lambda)^4$  and the absorption cross section is dependent upon  $(\pi D/\lambda)$ . At the temperatures typical of a combustion system the radiation is generally of a wavelength,  $\lambda$ , of  $1\mu\text{m}$  or higher. Hence, for small diameter,  $D$ , particles the scattering will be negligible compared to the absorption coefficient. For larger agglomerates and chains of particles this is not necessarily true. The assumption is made that the soot is made up of small particles in this study, and so scattering is neglected. The formulation then reduces to,

$$\frac{dI}{ds} = -k_a I + \frac{k_a \sigma T_g^4}{\pi} \quad (7)$$

Given a representative ray the intensity distribution can be calculated along it. This equation can be integrated to give the recurrence relationship,

$$I_{n+1} = \frac{\sigma T_g^4}{\pi} (1 - e^{-k_a \Delta s}) + I_n e^{-k_a \Delta s} \quad (8)$$

Thus the intensity may be calculated stepwise as the ray passes through successive control volumes within the domain. The initial intensity is calculated assuming that the surface is a gray, Lambert one,

$$I_0 = \frac{q_+}{\pi} = (1 - \varepsilon_w) \frac{q_-}{\pi} + \varepsilon_w \frac{\sigma T_w^4}{\pi} \quad (9)$$

Then at any given point on the boundary the incoming heat flux due to radiation is,

$$q_- = \int_{2\pi} I_w(\Omega) \cos \theta d\Omega \quad (10)$$

Clearly,  $q_-$  may only be calculated given knowledge of the initial intensity of the ray impinging on the surface of interest. Thus the process is iterative with updated initial ray intensities used at the beginning of each new iteration loop.

The net wall radiative heat flux is simply the difference between the energy flux away from the surface and towards the surface,

$$q_w = q_- - q_+ \quad (11)$$

The net radiation energy change in a control volume must be accounted for in the overall flow solution procedure's energy conservation equations. A source term is used to represent this change in energy. Once the ray intensities have been resolved the calculation of the

source terms follow with relative ease. The radiation source to a particular control volume for a single ray may be expressed as,

$$S = dA \cos \theta \Delta \Omega (I_{n+1} - I_n) \quad (12)$$

The contribution of each ray passing through the control volume must be summed to produce the overall control volume source term.

The integrals in the above equations are replaced by numerical quadrature in the application of the DT algorithm. In this way Eq. 10. is rewritten as,

$$q_- = \sum I_w(\Omega) \cos \theta \Delta \Omega \quad (13)$$

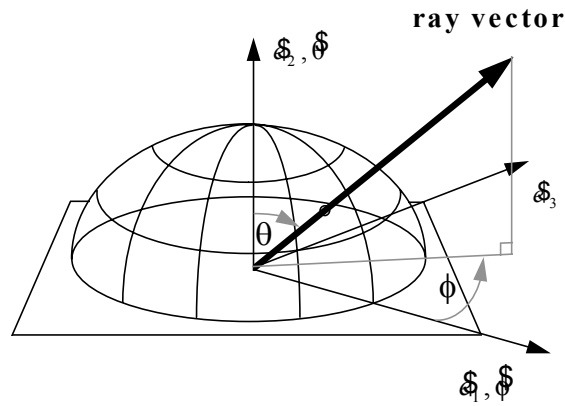


**Figure .2. Discretisation of a solid angle hemisphere**

The discretisation of the solid angle in Eq. 13. over a hemisphere has been addressed by a number of authors. Conventionally the solid angle hemisphere is discretised by equal division of polar and azimuthal angles (see Fig.2), and Eq. 13. becomes,<sup>12</sup>

$$q_- = \sum_{i=1}^{N_\theta} \sum_{j=1}^{N_\phi} I_w(\theta_i, \phi_j) (\cos \theta_i) (\sin \theta_i) (\sin \Delta\theta) \Delta\phi \quad (14)$$

where,

$N_\theta$  = number of rays in  $\theta$  direction,  $0 < \theta < \pi/2$

$N_\phi$  = number of rays in  $\phi$  direction,  $0 < \phi < 2\pi$

$\Delta\theta$  = solid angle increment in the  $\theta$  direction

$\Delta\phi$  = solid angle increment in the  $\phi$  direction

For constant  $\Delta\theta$  and  $\Delta\phi$  in Eq. 14. the weightings are proportional to  $\sin 2\theta$  which produces a bias to rays closest to  $\theta = \pi/4$ . A further limitation is that rays at an angle close to the surface have the same weighting as rays close to the normal direction from the surface. Improvements can be made by ensuring a more even distribution of ray directions.

The discretisation of the solid angle was addressed by Cumber.<sup>13</sup> Improvements in efficiency were obtained for a limited number of rays. A more detailed analysis has been performed by Bressloff et al, who compared results over a range of ray numbers.<sup>14</sup> A more uniform distribution of ray directions was obtained by realigning the co-ordinate axis, moving the poles away from the surface normal, and discretising the solid angle hemisphere to give approximately equal areas. Significant improvements in computational efficiency were made over a range of cases.

## Ray Tracing

The lengths of every segment of each ray through the control volumes making up the domain must be computed before any intensity calculation can be performed. The ray tracing calculation must account for the control volume geometry typical of the solver being used. Although the calculation is complex and time consuming it need only be performed once prior to the main solution procedure.

Each control volume surface may be described by an equation. A simplifying assumption of axisymmetry significantly reduces the amount of information that need be specified by the user. In this way each duct section requires the specification of only a single surface. Most combustors of interest match the requirement of axisymmetry. Non-axisymmetric geometries can be modelled using the procedure developed here by implementing some simple extensions to the underlying logic.

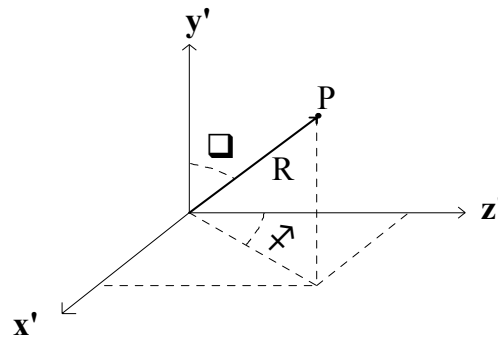


**Figure .3. Description of transformation from spherical to rectangular co-ordinate system**

Rays are launched from the axial midpoint of every volume boundary surface. The number of rays launched is user defined. The equations describing the rays are generated in

spherical co-ordinates about the midpoint, which is specified as the origin of the local frame of reference, see Fig. 3.

The equations may be transformed from spherical to Cartesian co-ordinates as follows,<sup>15</sup>

$$\begin{aligned} x' &= R \sin \theta \sin \phi \\ y' &= R \cos \theta \\ z' &= R \sin \theta \cos \phi \end{aligned} \tag{15}$$

where the ray is represented by the length  $R$  from the origin to point  $P$ .

The local co-ordinate system is then translated and rotated into the global co-ordinate system (see Fig. 4). In this way all the rays and surfaces are described in the exact same global Cartesian co-ordinate system.

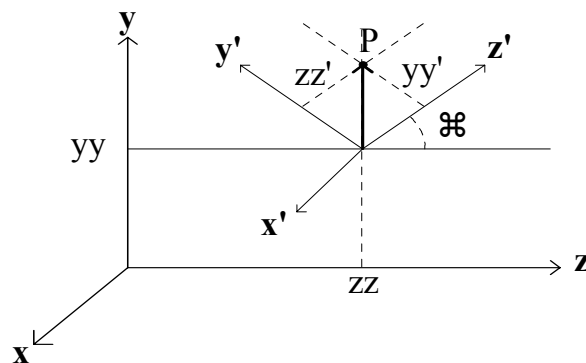


**Figure .4. Description of rotation and translation from local to global co-ordinate system**

The translation and rotation is represented as,

$$\begin{aligned}
x &= x' \\
y &= yy + yy' \cos \zeta + zz' \sin \zeta \\
z &= zz + zz' \cos \zeta - yy' \sin \zeta
\end{aligned}
\tag{16}$$

The equations describing the ray are now solved by simple substitution, and the result, written in parametric form in the global co-ordinate frame is,

$$\begin{aligned}
x &= (\sin \theta \sin \phi)t \\
y &= yy + (\sin \theta \cos \phi \sin \zeta + \cos \theta \cos \zeta)t \\
z &= zz + (\sin \theta \cos \phi \cos \zeta - \cos \theta \sin \zeta)t
\end{aligned}
\tag{17}$$

Thus a simple description of the ray is obtained dependent only upon its origin (the boundary surface mid-points) and the user specified polar and azimuthal angles. The boundary surfaces (planes, cylinders, and cones) must also be described by equations in the global Cartesian co-ordinate frame of reference.<sup>15</sup>

The procedure also allows sections of ducts to be ‘pasted’ together with rays passing freely between them, a requirement to model geometries such as double annular combustors.

## Radiative Properties

Radiative properties of combustion gases present a difficult obstacle in performing an accurate, reliable radiation calculation. The radiative properties are dependent upon temperature, pressure, composition, wavelength, and path length. The concentrations of the constituent species must first be predicted. This initial step typically introduces the largest errors into the calculation. The radiative properties of the constituents of each control volume are then calculated, which may include gross approximations especially in the soot properties calculation. The only alternative to performing these calculations is to match measured absorption coefficients to the combustor of interest, obviously greatly limiting the predictive capabilities of the code. The aim of the models developed in this work is to offer the user the capability of either specifying or computing the radiative properties.

The radiative transfer from an opaque wall can often be represented by a simple model of gray (having radiative properties which do not vary with wavelength) emission, absorption and reflection. Unfortunately, the same assumption cannot be made about a molecular gas, since the radiative properties vary significantly across the gas spectrum, and are strongly dependent upon wavelength. A detailed discussion and comparison of methods has been performed by Bressloff et al.<sup>16</sup>

The operating environment of a gas turbine combustor at elevated pressure severely restricts the selection of a gas properties model. Much of the work in this area has been performed at atmospheric pressure, or at least an order of magnitude lower pressure than that found in a typical gas turbine combustor. Unfortunately the effects of pressure broadening cannot be ignored, and models which account for them must rely on extrapolation.

In a system containing combustion gases the emission from the molecules of H<sub>2</sub>O and CO<sub>2</sub> dominate, and the effects of the remaining constituents are small enough to be assumed

negligible. Leckner developed and improved existing gas emissivity charts based on the integration of spectral data.<sup>17</sup> The formulation has a maximum error of 5% for water vapour, and 10% for carbon dioxide compared with the spectrally integrated intensities, for temperatures above 400 K. A clear concise of description of the model has been provided by Modest.<sup>5</sup>

The luminous component of radiation may far outweigh the non-luminous radiation in some areas of the combustor flametube, especially in the fuel rich pockets within the primary zone. At the high pressures present within the gas turbine combustor the soot particles attain sufficient size to radiate as black bodies.<sup>3</sup> When a parallel beam of radiation passes through a domain of particles the strength of the beam decreases exponentially as follows,<sup>3</sup>

$$\frac{I_{n+1}}{I_n} = \exp(-K\Delta s) \quad (18)$$

Assuming as previously (in formulation of DT) that the scattering is negligible,  $K$  is equivalent to the absorption coefficient. If the emissivity is equal to the absorptivity, the emissivity may be defined as,<sup>3</sup>

$$\varepsilon_s = \frac{I_n - I_{n+1}}{I_n} \quad (19)$$

Substituting from Eq. 21 the formulation may be rewritten as,

$$\varepsilon_s = 1 - \exp(-k_a \Delta s) \quad (20)$$

where,

$$k_a = \frac{3.72 f_v C_0 T}{C_2}$$

The above formulation is only applicable to situations where very small soot particles exist. The extinction coefficient will increase with increasing particle sizes. The value of  $C_0$  is taken to be 7.0.<sup>9</sup> Values range from 3 to 10 depending on the fuel type and test conditions.<sup>4</sup>

The process of soot formation and oxidation is extremely complex. Quantitatively accurate methods for calculating soot production within the operating regimes of a gas turbine combustor have yet to be developed. Soot is not an equilibrium product of combustion.<sup>18</sup> It depends upon physical processes such as atomisation, evaporation and turbulent mixing as much as the chemical kinetics.

The process of soot formation occurs in three stages: soot-particle nucleation, agglomeration and surface growth, and coagulation. The first step is the one least understood.

Quasi-global models have been developed to describe the process of soot formation. Najjar and Goodger developed a successful model after studying soot formation in a gas turbine combustor burning kerosene and gas oil.<sup>19</sup> Soot oxidation tends to dominate in the regions downstream of the primary zone, at lower fuel/air ratios, and correspondingly higher temperatures. Mongia supplemented empirical data into multi-dimensional calculations to predict the sooting process of formation and oxidation within a gas turbine combustor.<sup>20</sup> Sudarev and Antonovsky developed a formulation for soot concentration based on a detailed experimental study of a class of combustors.<sup>21</sup> The accuracy of these models becomes limiting as the operating conditions of the combustor differ significantly from the regime of the formulation of the correlation.

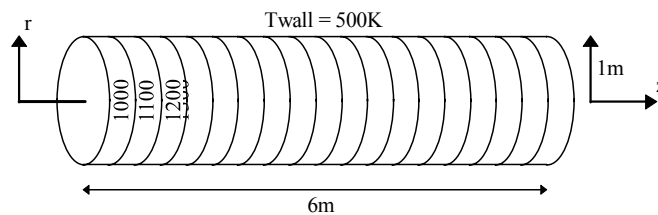
Once the soot and gas emissivities have been computed the effective total emissivity may be obtained from the following,

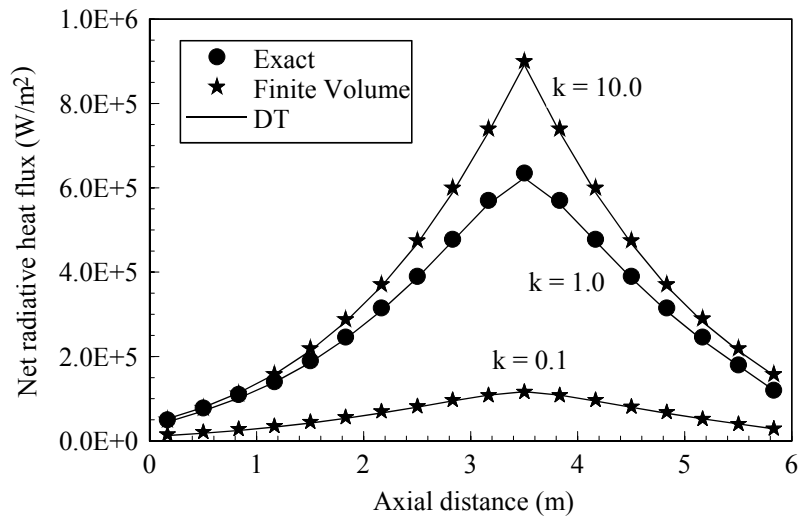
$$\epsilon_T = \epsilon_g + \epsilon_s - \epsilon_g \epsilon_s \quad (21)$$

The total emissivity calculated using Eq. 21 has been found to give good agreement with values computed using a more detailed non-gray analysis.<sup>3</sup>

### **Validation of Discrete Transfer Radiation Model**

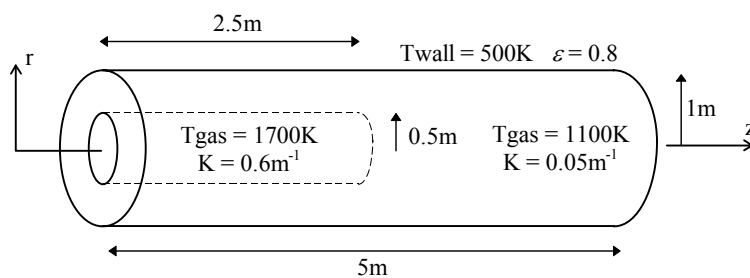
Malalasekera and James performed radiation calculations in three-dimensional complex geometries using the DT method.<sup>22</sup> The accuracy of their model was successfully evaluated using the results of Chui et al.<sup>23</sup> The geometry used is shown in Fig. 5. The cylindrical enclosure is 6m long and 2m in diameter. The walls are black at a constant uniform temperature of 500K. The gas temperature varied axially along the cylinder, as shown in Fig. 5. The results shown in Fig. 5 were obtained for three different absorption coefficients, using an exact calculation, and the finite volume method of Chui et al.<sup>23</sup>





**Figure .5. Radiative flux comparison on cylinder**

The flowfield used in the overall network calculation is only one-dimensional. This is a severe limitation when computing radiative transfer, as radial variations in temperature and properties might significantly affect the radiation in real situations. User specified profiles have been incorporated allowing the DT calculation to be performed taking into account the radial variations in the gas. The profiles may be either absolute values or non-dimensional values about the computed mean obtained from the network solver. The profiles may be derived from two sources, either user defined based on experience, or from experimental and CFD analysis of a particular combustor.



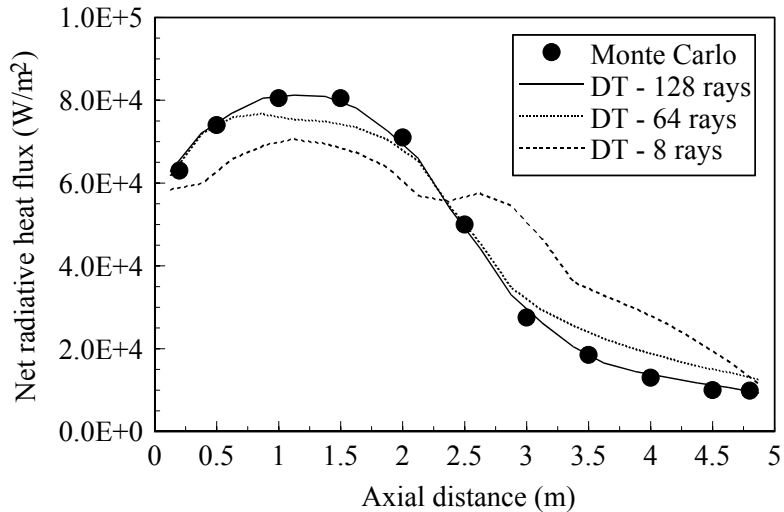


**Figure .6. Comparison of radiative flux on cylinder**

The overall profiles within the combustor should remain relatively similar over a broad range of operating conditions.

The second validation case included a radial variation in temperature and properties.<sup>12</sup> The geometry considered consisted of a finite cylinder 5m long and 2m in diameter. The walls are at a temperature of 773K and an emissivity of 0.8. The gas contains a hot region at a temperature of 1700K and an absorption coefficient of  $0.6\text{m}^{-1}$ . The remainder of the cylinder is at a temperature of 1100K and an absorption coefficient of  $0.05\text{m}^{-1}$ , as shown in Fig. 6. Comparisons were made between a detailed accurate Monte Carlo calculation and the DT calculation using 8, 64, and 128 rays (see Fig. 6.).

The importance of using a sufficient number of rays is clearly illustrated. If too few rays are used the calculation suffers from the ‘ray effect’. The number of representative rays used must capture variations in the gas temperature and properties. This may lead to problems in gases with steep gradients as the rays may completely miss a peak value.

## **Gas Turbine Combustor Evaluation**

The annular combustor shown in Fig. 7. was selected to evaluate the effects of the new radiation modelling approach on the predicted liner wall temperatures. The large amount of experimental and computational data available on this combustor made it an attractive source for validation of the various models.

The dark outline is a not to scale representation of the combustor general features. The solid network of elements and nodes refers to the flow computational cells, in which the flow and energy equations are solved. The dashed network represents the heat transfer sequence of elements and nodes required to model the overall heat transfer from the flametube through the liner to the annuli.

Mass flow splits, and pressure-drops were computed in the flow logic links, and included appropriate correlations for diffuser, liner hole features, and duct flows. The mixing and recirculation models were used to compute local bulk fuel/air ratios for a constrained equilibrium calculation. The heat transfer logic allows for the effects of film cooling, thermal barrier coating, and liner feature heat pick-up. Heat transfer through the double skin regions was also computed. Radial profiles of temperature and soot were included in the radiation calculation within the flametube. These profiles were obtained from predictions compared with measurements taken within a combustor flametube.<sup>24</sup>

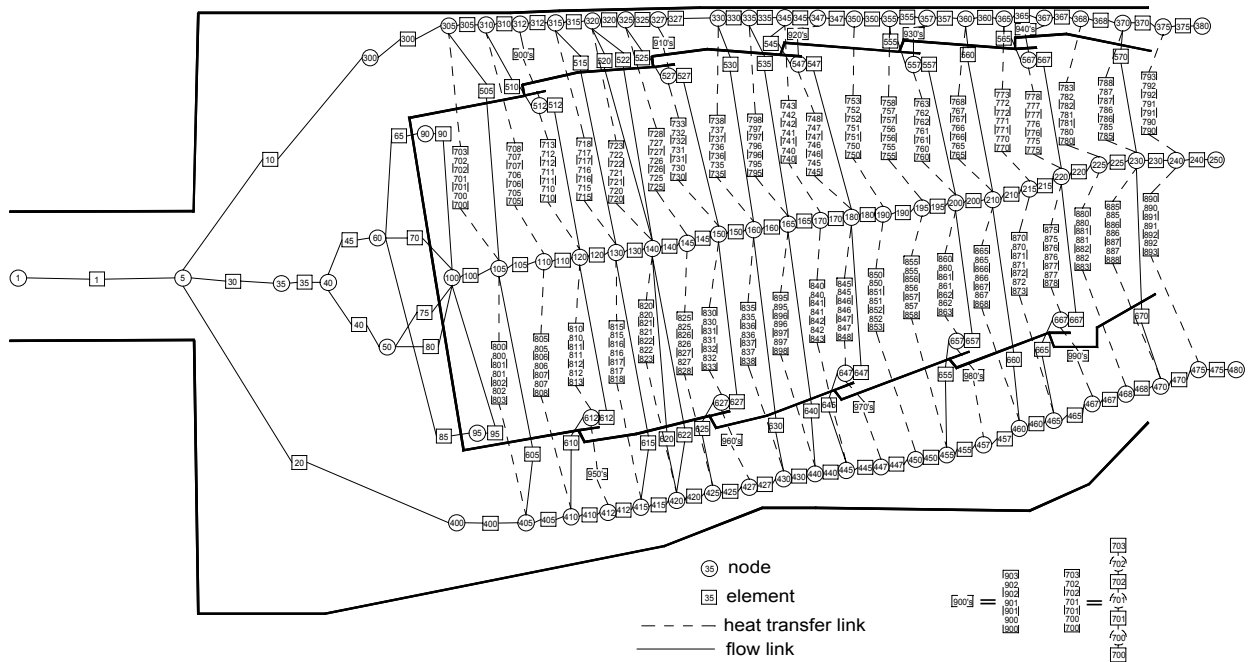
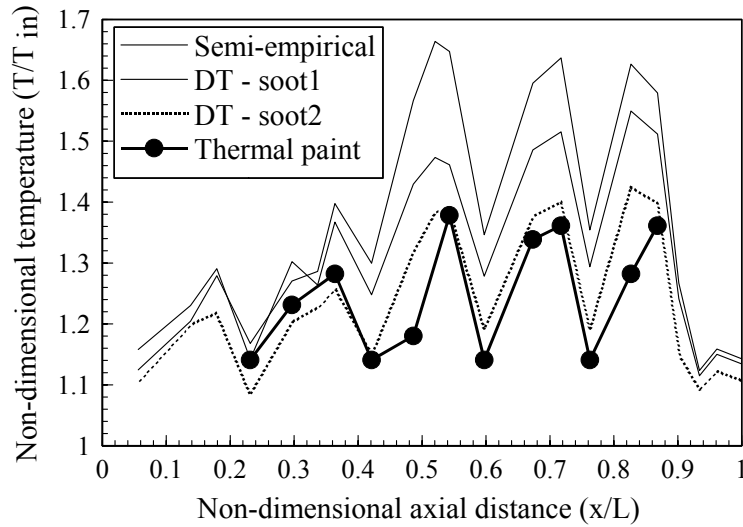


Figure .7. Network diagram for annular combustor case study

## Results and Discussion

The network solver has been previously validated against a number of annular and reverse flow combustors.<sup>1</sup> The solver demonstrated accuracy and versatility in modelling complex geometries. A limitation of the solver was in its ability of predicting the radiative fluxes within the combustor flametube.<sup>1</sup>



**Figure .8. Annular combustor outer annulus liner wall temperature comparison**

Thermal barrier coating hot side experimental thermal paint data was provided as a basis for the wall temperature comparisons on the annular combustor shown in Fig. 7.<sup>25</sup>

Comparisons between experimental measurements and predicted wall temperatures are shown in Fig. 8. and Fig. 9.

The ‘Semi-empirical’ prediction uses a simple semi-empirical calculation based on the bulk gas properties at a particular axial location for computing the radiative flux.<sup>3</sup>

The ‘DT - soot1’ prediction involves a full discrete transfer radiation model of the combustor flametube. The model utilises circumferentially averaged radial profiles of temperature and soot volume fraction. The soot volume fractions in this case used a model incorporating measurements in a confined turbulent jet flame.<sup>24</sup> The model does not correctly compute the oxidation of soot and hence the soot concentrations are one or two orders of magnitude higher than measured values.

The ‘DT - soot2’ prediction uses the same temperature profile as the previous prediction but the soot profile is derived from a model incorporating detailed reaction kinetics.<sup>24</sup> The soot volume fractions in this case compared more closely with the measured data.

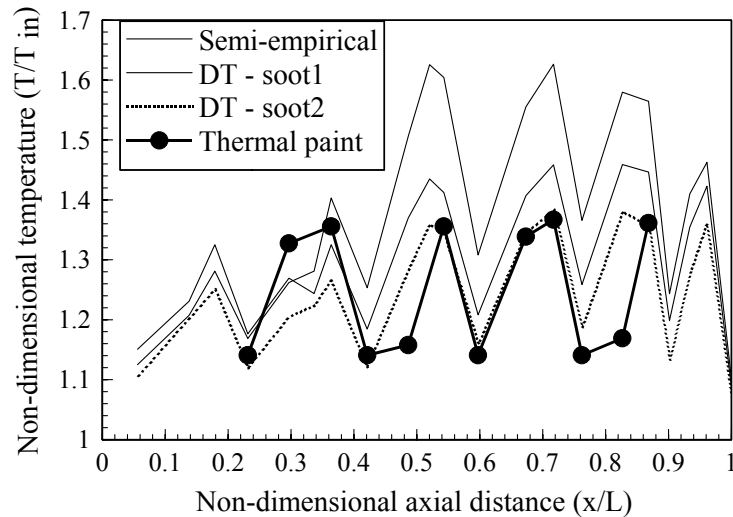


**Figure .9. Annular combustor inner annulus liner wall temperature comparison**

The ‘soot2’ prediction provided a moderately better comparison with wall temperatures than the ‘soot1’ calculation. The maximum difference between the ‘soot2’ prediction and the thermal paint measurements was 80K. However, the difference was much less than this over most of the inner and outer annulus liner walls. The trends of the prediction closely matched those of the measurements.

The increased levels of soot in the ‘soot1’ prediction resulted in a higher liner wall temperature than the ‘soot2’ data, as expected. However, the lower gas temperatures adjacent to the liner wall may result in the cooler soot shielding the wall. If the soot profiles are flat as in ‘soot1’ this effect is strengthened.

The error in the experimental measurements ranges from 20K in the hottest regions to 100K in the cooler regions. The thermal paint data consists of discrete point values which have been joined for clarity as plotted in Fig. 8. and Fig. 9.

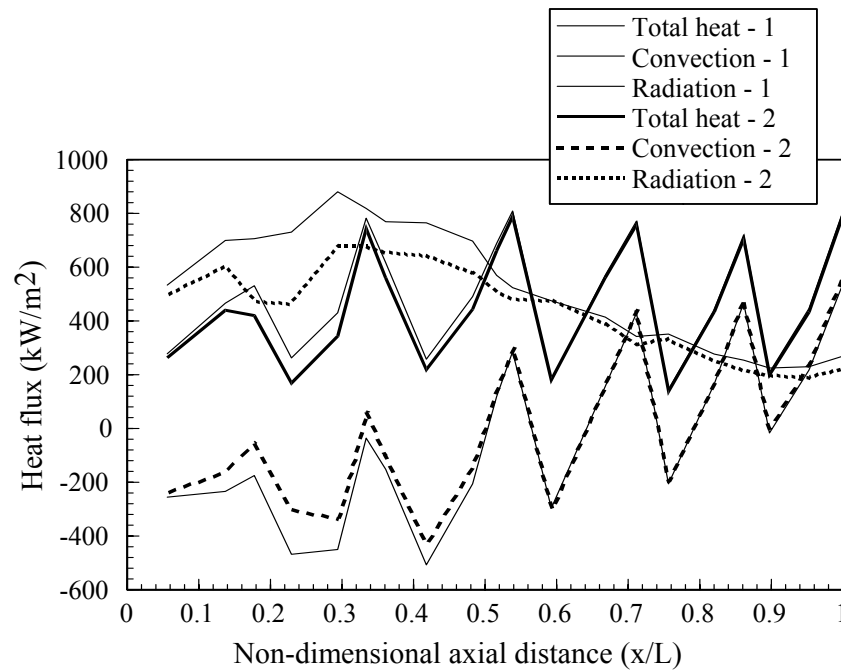


**Figure .10. Annular combustor outer annulus liner wall profile heat flux comparison**

The axial location of the measurement points was not precise between bay end points. Thus the discrepancies in these temperature points (at 0.49 on the outer wall, and 0.49 and 0.84 on the inner liner) were not of concern. Furthermore, the error bands in the measurements in this temperature range were 100K. The maximum measured temperatures do fall within the narrow 20K error band on both the inner and outer liner wall.

When designing a combustor it is unlikely that sufficient information will be available to generate temperature and soot profiles within the flametube. Fig. 10 examines the sensitivity of the conjugate heat transfer for a given profile of soot and temperature, and corresponding

bulk values, i.e. no profile. The curves designated '1' represent a single bulk soot and temperature, while the curves designated '2' make use of the profiles. The primary zone fluxes were most effected by this simplification. Since the walls are film cooled the increasing negative convective flux somewhat compensates the increasing radiative flux. The maximum difference in predicted wall temperatures between the two cases is 60K in the primary zone.

The importance of non-luminous effects were also evaluated. In regions of lower soot concentration, downstream of the primary zone the gas component of emission is not necessarily negligible. The effects are of course dependent upon the soot levels within a particular combustor.

Further details of the combustor radiation interaction and the underlying network strategy may be found in Stuttford.<sup>26</sup>

## **Conclusions**

A radiation model was implemented and evaluated within a proven preliminary gas turbine combustor preliminary design algorithm.

Although the radiation model is accurate it relies on a description of the combustor flowfield derived from experimental data or detailed computational fluid dynamics calculations. Physically realistic assumptions may be used if such data is not available, still providing a model more accurate than a simple semi-empirical calculation. The improved network model was able to closely match the wall temperature trends in an annular combustor. The model also provided a reasonable match on the magnitudes of liner temperature.

The incorporation of the discrete transfer radiation model provides a versatility and accuracy comparable to the underlying network algorithm.

### **Acknowledgements**

This work was funded and supported by Rolls-Royce plc and the Defence Research Agency, with valuable technical input from both organisations.

### **References**

1. Stuttaford, P.J. and Rubini, P.A., 1996, "Preliminary Gas Turbine Combustor Design Using a Network Approach", *ASME Paper no. 96-GT-135*, to appear in the *Journal of Engineering for Gas Turbines and Power*.
2. Greyvenstein, G.P. and Laurie, D.P., 1994, "A Segregated CFD Approach to Pipe Network Analysis", *International Journal for Numerical Methods in Engineering*, Vol. 37, pp. 3685-3705.
3. Lefebvre, A.H., 1984, "Flame radiation in gas turbine combustion chambers", *International Journal of Heat and Mass Transfer*, Vol. 27, No. 9, pp. 1493-1510.
4. Siegel, R. and Howell, J.R., 1992, "Thermal Radiation Heat Transfer, Third Edition", Hemisphere Publishing Corporation, U.S.A.
5. Modest, M.F., 1993, "Radiative Heat Transfer", McGraw-Hill Inc., U.S.A.
6. Viskanta, R. and Menguc, M.P., 1987, "Radiation Heat Transfer in Combustion Systems", *Progress in Energy and Combustion Science*, Vol. 13, pp. 97-160.

7. Lockwood, F.C. and Shah, N.G., 1981, "A New Radiation Solution Method for Incorporation in General Combustion Prediction Procedures", *Proceedings of the Eighteenth Symposium (International) on Combustion*, pp. 1405-1414.
8. Rizk, N.K. and Mongia, H.C., 1991, "Three-Dimensional Analysis of Gas Turbine Combustors", *Journal of Propulsion and Power*, Vol. 7, No. 3, pp. 445-451.
9. Menguc, M.P., Cummings, W.G. and Viskanta, R., 1985, "Radiative Transfer in a Gas Turbine Combustor", *AIAA Paper no. AIAA-85-1072*.
10. Carvalho, M.G. and Coelho, P.J., 1989, "Heat Transfer in Gas Turbine Combustors", *Journal of Thermophysics*, Vol. 3, No. 2, pp. 123-131.
11. Bai, X.S. and Fuchs, L., 1994, "Numerical Computation of Turbulent Combustion and Thermal Radiation in Gas Turbine Combustion Chambers", *ICAS-94-6.6.1*, pp. 2098-2106.
12. Shah, N.G., 1979, "New Method of Computation of Radiant Heat Transfer in Combustion Chambers", PhD Thesis, University of London.
13. Cumber, P.S., 1995, "Improvements to the Discrete Transfer Method of Calculating Radiative Heat Transfer", *International Journal of Heat and Mass Transfer*, Vol. 38, No. 12, pp. 2251-2258.
14. Bressloff, N.W., Moss, J.B., Rubini, P.A., 1995, "Application of a New Weighting Set for Discrete Transfer Radiation Model", *Proceedings of the 3rd European Conference on Industrial Furnaces and Boilers*, Lisbon, Portugal.
15. Kindle, J.H., 1950, "Theory and Problems of Plane and Solid Analytic Geometry", Schaum's Outline Series, McGraw-Hill Book Company, U.S.A.
16. Bressloff, N.W., Moss, J.B., Rubini, P.A., 1996, "Assessment of a Differential Total Absorptivity Solution to the Radiative Transfer Equation as Applied in the Discrete Transfer Radiation Model", *Numerical Heat Transfer, Part B*, Vol. 29, No. 3, pp. 381-397.

17. Leckner, B., 1972, "Spectral and Total Emissivity of Water Vapour and Carbon Dioxide", *Combustion and Flame*, Vol. 19, pp. 33-48.
18. Srivasta, S.K., 1982, "Computations of soot and NO<sub>x</sub> emissions from Gas Turbine Combustors", *NASA CR-167930*, U.S.A.
19. Najjar, Y.S.H. and Goodger, E.M., 1981, "Soot formation in gas turbines using heavy fuels. 1.", *Fuel*, Vol. 60, pp. 980-986.
20. Mongia, H.C., 1994, "Combustor Modelling in Design Process: Applications and Future Directions", *AIAA Paper no. AIAA-94-0466*.
21. Sudarev, A.V. and Antonovsky, V.I., 1990, "Soot Content in a Gas Turbine Combustion Chamber", *Low Grade Fuels*, Vol. 2, Ch. 36, pp. 431-441.
22. Malalasekera, W.M.G. and James, E.H., 1996, "Radiative Heat Transfer Calculations in Three-Dimensional Complex Geometries", *Journal of Heat Transfer*, Vol. 118, pp. 225-228.
23. Chui, E.H., Hughes, P.M.J. and Raithby, G.D., 1993, "Implementation of the Finite Volume Method for Calculating Radiative Heat Transfer in a Pulverized Fuel Flame", *Combustion Science and Technology*, Vol. 92, pp. 225-242.
24. Brocklehurst, H.T., Priddin, C.H. and Moss, J.B., 1997, "Soot Predictions within an Aero Gas Turbine Combustion Chamber", to appear in *ASME/IGTI Turbo Expo '97*, Orlando, U.S.A.
25. Metcalfe, M., 1996, Private Communication, Rolls-Royce plc, U.K.
26. Stuttaford, P.J., 1997, "Preliminary Gas Turbine Combustor Design Using a Network Approach", PhD Thesis, Cranfield University, England, to appear March 1997.